JOURNAL OF VIROLOGY, Apr. 1994, p. 2388–2397
0022-538X/94/$04.00+0

Vol. 68, No. 4

The Tobacco Etch Potyvirus 6-Kilodalton Protein Is Membrane Associated and Involved in Viral Replication

MARÍA A. RESTREPO-HARTWIG AND JAMES C. CARRINGTON*
Department of Biology, Texas A&M University, College Station, Texas 77843

Received 20 September 1993/Accepted 12 January 1994

The tobacco etch potyvirus (TEV) genome encodes a polyprotein that is processed by three virus-encoded proteinases. Although replication of TEV likely occurs in the cytoplasm, two replication-associated proteins, VPg-proteinase (nuclear inclusion protein a) (NIa) and RNA-dependent RNA polymerase (nuclear inclusion protein b) (NIb), accumulate in the nucleus of infected cells. The 6-kDa protein is located adjacent to the N terminus of NIa in the TEV polyprotein, and, in the context of a 6-kDa protein/NIa (6/NIa) polyprotein, impedes nuclear translocation of NIa (M. A. Restrepo-Hartwig and J. C. Carrington, J. Virol. 66:5662–5666, 1992). The 6-kDa protein and three polyproteins containing the 6-kDa protein were identified by affinity chromatography of extracts from infected plants. Two of the polyproteins contained NIa or the N-terminal VPg domain of NIa linked to the 6-kDa protein. To investigate the role of the 6-kDa protein in vivo, insertion and substitution mutagenesis was targeted to sequences coding for the 6-kDa protein and its N- and C-terminal cleavage sites. These mutations were introduced into a TEV genome engineered to express the reporter protein β-glucuronidase (GUS), allowing quantitation of virus amplification by a fluorometric assay. Three-amino-acid insertions at each of three positions in the 6-kDa protein resulted in viruses that were nonviable in tobacco protoplasts. Disruption of the N-terminal cleavage site resulted in a virus that was approximately 10% as active as the parent, while disruption of the C-terminal processing site eliminated virus viability. The subcellular localization properties of the 6-kDa protein were investigated by fractionation and immunolocalization of 6-kDa protein/GUS (6/GUS) fusion proteins in transgenic plants. Nonfused GUS was associated with the cytosolic fraction (30,000 × *g* centrifugation supernatant), while 6/GUS and GUS/6 fusion proteins sedimented with the crude membrane fraction (30,000 × *g* centrifugation pellet). The GUS/6 fusion protein was localized to apparent membranous proliferations associated with the periphery of the nucleus. These data suggest that the 6-kDa protein is membrane associated and is necessary for virus replication.

Tobacco etch virus (TEV) belongs to the potyvirus group, one of the largest and most damaging groups of plant viruses. The virion consists of a positive-strand RNA of 9,495 nucleotides (nt) containing a virus-encoded protein (VPg) attached covalently to the 5′ end and over 2,000 copies of a coat protein subunit (1, 45). The viral genome encodes a large polyprotein that is processed by three virus-encoded proteinases to yield the mature products. Two proteinases, P1 and the helper component proteinase (HC-Pro), catalyze only autoproteolytic reactions at their respective C termini (7, 53). The remaining cleavage reactions are catalyzed by either *trans*-proteolytic or autoproteolytic mechanisms by the small nuclear inclusion protein (NIa), an evolutionary homolog of the picornavirus 3C proteinase (8, 9).

Several TEV proteins, including the cylindrical inclusion protein (CI), NIa, and the large nuclear inclusion protein (NIb), have been postulated to perform direct roles in viral RNA replication. By using plum pox potyvirus, the CI protein was shown to possess RNA helicase and ATPase activities (29, 30). The multifunctional NIa protein, besides functioning as a proteinase, serves as the VPg (36, 37, 44, 48). In a proportion of NIa molecules in vivo, a self-cleavage reaction occurs between the N-terminal VPg and the C-terminal proteinase domains at a suboptimal processing site (19). On the basis of sequence similarities with other positive-strand RNA viruses, NIb was proposed to be the RNA-dependent RNA polymerase (1, 16). The CI protein accumulates in the cytoplasm, while NIa and NIb accumulate mainly in the nucleus, although the pool of NIa linked to viral RNA as VPg is found in virions in the cytoplasm (3, 4, 31, 41, 50). Between CI and NIa in the viral polyprotein is the putative 6-kDa protein, a small polypeptide whose existence is inferred by the presence of functional NIa-mediated cleavage sites (6, 8). The 6-kDa protein has yet to be detected in vivo either as a mature product or as part of a polyprotein. Furthermore, little information concerning the function of this protein during virus infection is available. However, in transgenic plants expressing 6-kDa protein/NIa (6/NIa) polyproteins, the 6-kDa protein inhibits the nuclear translocation activity of NIa (42), suggesting that the small polypeptide may play a regulatory role in subcellular transport of NIa.

Potyviruses belong to the picornavirus supergroup of positive-strand RNA viruses (14, 49). These viruses encode a polyprotein containing a conserved series of domains that include the VPg, the 3C-like proteinase, and the RNA polymerase. In the picornavirus polyprotein, a membrane-binding protein termed 3A is located immediately upstream of the VPg (protein 3B) (46, 51, 52). The 3A protein, which is found predominantly in the form of a 3AB polyprotein, is proposed to serve as a membrane-binding anchor for the VPg during initiation of RNA synthesis (20, 21, 51). The fact that the potyviral 6-kDa protein is adjacent to the VPg domain provokes the idea that this protein may provide a function similar to that of the picornaviral 3A protein. A putative membrane-binding function for the 6-kDa protein may explain its ability to inhibit NIa-mediated nuclear translocation.

The objectives of the present study were to identify the 6-kDa protein and 6-kDa-protein-containing polyproteins in

* Corresponding author. Phone: (409) 845-2325. Fax: (409) 845-2891. Electronic mail address: carrington@bio.tamu.edu.

virus-infected cells, to test the hypothesis that the 6-kDa protein is involved in viral RNA amplification, and to analyze the subcellular localization properties of the 6-kDa protein. A histidine tag was introduced at the N terminus of the 6-kDa protein through engineering of a full-length TEV infectious clone, enabling concentration of the 6-kDa protein from infected tissue by affinity chromatography. A mutational analysis targeting the 6-kDa protein and its cleavage sites was conducted to assess the role of the 6-kDa protein in replication in the protoplast cell culture system. Finally, the subcellular localization properties of the 6-kDa protein were analyzed by fractionation and immunogold labeling studies with transgenic plants expressing fusion polypeptides containing the 6-kDa protein.

MATERIALS AND METHODS

Plants and antisera. *Nicotiana tabacum* cv. Xanthi nc was used for virus infections, protoplast isolation, preparation of transgenic plants, and isolation of inclusion bodies. CI protein and NI bodies were purified according to the method of Dougherty and Hiebert (18). The anti-NIa, anticapsid, and anti-CI sera were described previously (41). A synthetic peptide consisting of TEV amino acids 1797 to 1849, corresponding to the complete 6-kDa protein, was prepared at the Biotechnology Support Laboratory—Peptide Services at Texas A&M University. Monospecific antiserum against the synthetic 6-kDa protein was produced in New Zealand White rabbits by the method of Harlow and Lane (22). Anti-β-glucuronidase (anti-GUS) serum was kindly provided by Tom McKnight (Texas A&M University).

Construction of plasmids. The plasmid pTL7SN-CI/6/pNIa contains TEV sequences (nt 3634 to 5916) corresponding to the coding sequence for the CI protein, the 6-kDa protein, and NIa amino acid residues 1 to 74. Sequences coding for seven His residues were inserted by site-directed mutagenesis (27) between the first and second codons of the 6-kDa protein sequence, generating pTL7SN-CI/His6/pNIa. The *Eco*NI-*Bam*HI fragment, corresponding to TEV nt 5468 to 5916 and containing the 7-His-residue insertion, was transferred to pTEV7DA to produce pTEV7DA-His6 (Fig. 1A).

The CAA codons at nt 5530 to 5532 and 5689 to 5691 were changed individually or in combination to GAC in pTL7SN-CI/6/pNIa. These mutations resulted in substitution of Asp for Gln in the P1 positions of the CI/6 and 6/NIa cleavage sites, respectively. The mutants carrying these substitutions were denoted by adding a D after the name of the protein affected by the change (CID, 6D, or CID/6D).

The sequence AGT-CGA-CCA coding for Ser-Arg-Pro was inserted in frame at three positions in the 6-kDa protein coding region in pTL7SN-5471, which contains TEV nt 5412 to 7098. Insertions were generated after TEV nt 5559, 5613, and 5643, resulting in plasmids designated by the suffixes 6KSal1, 6KSal2, and 6KSal3, respectively. Each mutation was introduced into pTEV7DA-GUS by transfer of an *Eco*NI-*Bam*HI fragment containing TEV nt 5468 to 5916. The plasmid pTEV7DA-GUS contains a full-length copy of the TEV genome downstream from a bacteriophage SP6 promoter and the sequence for GUS inserted between the P1 and HC-Pro coding regions (15).

The plasmid pGA-GUS/6 was used to prepare transgenic plants. The 6-kDa protein coding sequence was fused to the 3′ end of the GUS sequence in the vector pRTL2 by using a common *Bgl*II site, forming pRTL2-GUS/6. This plasmid contains the cauliflower mosaic virus 35S promoter and polyadenylation signals and the TEV 5′ nontranslated region. The entire expression cassette was excised by *Hin*dIII digestion and inserted in the binary vector pGA482 (2), creating pGA-GUS/6.

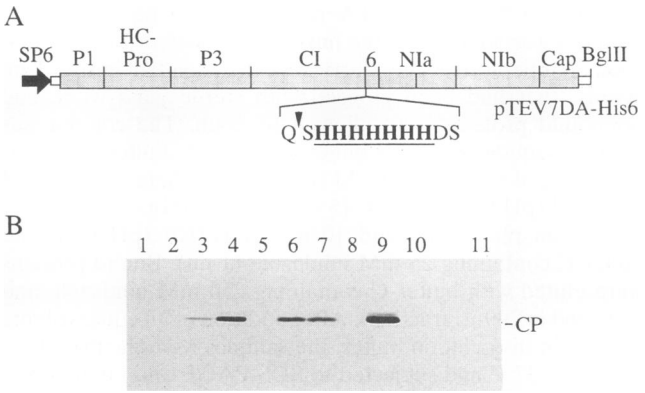

FIG. 1. Insertion of a His tag into the TEV genome. (A) Relevant portions of pTEV7DA-His6 from which infectious TEV RNA transcripts were generated. Sequences coding for polyprotein cleavage sites are indicated by vertical lines. The junction sequence between the CI protein and the 6-kDa protein, including the seven His residues (underlined) added by site-directed mutagenesis, is indicated below the map. The NIa-mediated processing site is indicated by an arrow. (B) Detection of TEV capsid protein in plants inoculated with pTEV7DA-His6 transcripts. Total SDS-soluble proteins were resolved by SDS-PAGE and subjected to immunoblot analysis with anticapsid serum. Lanes: 1 to 10, extracts from individual plants inoculated with pTEV7DA-His6 transcripts; 11, extract from a noninoculated plant. The position of the capsid protein (CP) is indicated on the right. Abbreviations: SP6, promoter for SP6 RNA polymerase; Cap, capsid protein; BglII, *Bgl*II restriction site.

In vitro transcription, in vitro translation, and protoplast inoculation. Plasmids used for in vitro transcription were purified by cesium chloride gradient centrifugation. Synthesis of transcripts with bacteriophage SP6 RNA polymerase (Ambion) for use in cell-free translation was as described elsewhere (42). Translation with rabbit reticulocyte lysates was done according to the manufacturer's (Promega) instructions. Production of m^7GpppG-capped transcripts from pTEV7DA, pTEV7DA-GUS, and their mutagenized derivatives was as described elsewhere (15). Concentration of transcripts and preparation and harvesting of protoplasts were as published elsewhere (12). Equivalent amounts of transcripts (~10 μg) were introduced into 5.0×10^5 protoplasts by polyethylene glycol-mediated transfection (38). Measurement of GUS activity was as described previously (10, 25).

Inoculation of plants. Transcripts were diluted in an equal volume of reaction buffer and used for inoculation immediately after in vitro transcription (15). At 7 days postinoculation (p.i.), systematically infected leaves were harvested, ground in 10 volumes of dissociation buffer, and subjected to sodium dodecyl sulfate-polyacrylamide gel electrophoresis (SDS-PAGE) and immunoblot analysis with anticapsid serum. Some of the plants inoculated with transcripts from pTEV7DA or pTEV7DA-His6 were ground in buffer A (6 M guanidine-HCl, 0.1 M sodium phosphate, and 10 mM Tris-HCl [pH 8.0]) and used for Ni^{2+}-nitrilotriacetic acid (NTA) affinity chromatography of protein extracts.

Affinity chromatography of His-tagged proteins on Ni^{2+}-NTA resin. Total protein extracts from virus-infected leaves (30 g) were prepared by grinding tissue in buffer A (60 ml) and stirred at room temperature for 1 h. Cell walls and debris were removed by filtration through eight layers of cheesecloth followed by centrifugation at 10,000 × *g* for 15 min at 4°C. One

milliliter of 50% Ni^{2+}-NTA resin (Qiagen) equilibrated in buffer A was added, and the mixture was stirred for 45 min at room temperature. The slurry was then loaded into a 1-ml syringe that had been plugged with sterile glass wool, and nonbound proteins were allowed to drain. The column was washed sequentially with buffer A (10 ml); buffer B (5 ml) consisting of 8 M urea, 0.1 M sodium phosphate, and 10 mM Tris-HCl (pH 8.0); buffer C (5 ml) composed of 8 M urea, 0.1 M sodium phosphate, and 10 mM Tris-HCl (pH 6.3); and buffer C containing 25 mM imidazole (1 ml). Bound proteins were eluted with buffer C containing 250 mM imidazole and collected in 200-μl fractions. After addition of an equal volume of protein dissociation buffer, the samples were incubated for 10 min at 37°C and subjected to SDS-PAGE and immunoblot analysis using anti-6-kDa-protein, anti-CI, and anti-NIa sera as described elsewhere (41).

Transgenic plants. Transgenic plants expressing nonfused GUS and 6/GUS fusion protein have been documented elsewhere (42). Transgenic plants expressing GUS/6 fusion protein were generated by using pGA-GUS/6 as described previously (41).

Subcellular fractionation. Leaf extracts were fractionated by differential centrifugation according to the method of Quadt and Jaspers (40), with some modifications. Tissue (1.5 g) from transgenic plants expressing GUS or 6/GUS or GUS/6 fusion protein were ground in the presence of glass beads in buffer Q (3 ml) consisting of 50 mM Tris-HCl, 15 mM $MgCl_2$, 10 mM KCl, 20% (vol/vol) glycerol, 0.1% (vol/vol) β-mercaptoethanol, 1 μM leupeptin, and 50 μM aprotinin (pH 7.4). Intact cells, nuclei, plastids, and cell debris were removed by sedimentation at 3,000 × *g* for 10 min at 4°C. The supernatant was subjected to centrifugation at 30,000 × *g* for 30 min at 4°C to separate the cytosolic fraction (supernatant S30) from the crude membrane fraction (pellet P30). The P30 fraction was resuspended in buffer Q (3 ml), and Nonidet P-40 (NP-40) (1%) was added to a portion to solubilize the membranes. The NP-40-solubilized and insoluble fractions were separated by centrifugation at 30,000 × *g* for 30 min at 4°C. Tissue equivalents from each fraction were analyzed for GUS activity by a fluorometric assay (10, 25).

Immunolocalization of the 6-kDa protein. Leaf tissue from 2-cm-tall transgenic plants expressing GUS or GUS/6 fusion protein was cut into small pieces (3 by 1 mm) and fixed in 4% formaldehyde–0.125% glutaraldehyde–50 mM potassium phosphate (pH 7.2) for 1.5 h at room temperature. Following washes in 50 mM potassium phosphate (pH 7.2), the specimens were dehydrated in an ethanol series (10, 30, 50, 70, 90, and 100%). The leaf pieces were embedded in LR White resin and polymerized by heating at 55°C for 24 h. Thin sections (silver-gold in color) were cut with an LKB Ultracut E Ultramicrotome and collected onto nickel grids coated with 2% collodion. Sections were blocked for 1 h with 2% bovine serum albumin (BSA) in TTBS (10 mM Tris-HCl, 0.05% Tween 20, 0.15 M sodium chloride, 0.02% sodium azide [pH 7.4]) containing 1% goat serum. The sections were then incubated for 2 h with 2% BSA-TTBS containing 1% anti-GUS or preimmune serum, washed repeatedly with 2% BSA-TTBS, and incubated for 1 h with goat anti-rabbit immunoglobulin G conjugated to 10-nm gold particles diluted 1:10 in 2% BSA-TTBS. The grids were rinsed first in TTBS and then in deionized water. Poststaining of sections was done with 2% aqueous uranyl acetate for 5 min and with Reynolds lead citrate (43) for 30 s before the sections were viewed on a Zeiss 10C transmission electron microscope.

RESULTS

Detection of the 6-kDa protein and polyproteins in TEV-infected plants. A polyclonal antiserum was raised against a synthetic version of the 6-kDa protein. By an immunoblot analysis after SDS-PAGE, this antiserum recognized the synthetic polypeptide but failed to react specifically with proteins in total extracts from TEV-infected leaves (data not shown). To facilitate detection of the 6-kDa protein and its putative polyprotein precursors from infected leaf tissue, a variant of TEV was engineered to allow affinity purification. The sequence coding for seven His residues was inserted after the first codon in the 6-kDa protein region in pTEV7DA (Fig. 1A), a plasmid containing a full-length TEV cDNA and from which infectious transcripts can be synthesized with SP6 RNA polymerase (12). The His tag enables binding to an affinity matrix containing immobilized Ni^{2+} (24).

To determine whether the addition of seven His residues to the 6-kDa protein affected TEV infectivity, tobacco plants were inoculated with transcripts from the modified plasmid (pTEV7DA-His6). Extracts prepared from plants 7 days p.i. were subjected to immunoblot analysis with anticapsid serum. In 5 of 10 plants, capsid protein was detected in upper, noninoculated leaves (Fig. 1B), indicating that the virus was competent for replication and systemic movement. The 50% infection efficiency with the pTEV7DA-His6 transcripts was similar to that of transcripts from the parental plasmid, pTEV7DA (data not shown).

Total guanidine-HCl-solubilized proteins from wild-type TEV- and TEV-His6-infected leaves were applied to an Ni^{2+}-NTA column, and bound proteins were eluted with imidazole-containing buffer. Two consecutive elution fractions were subjected to SDS-PAGE and immunoblot analysis with anti-6-kDa-protein, anti-CI, and anti-NIa sera. Two criteria were used to confirm that polypeptides detected by this method contained the 6-kDa protein sequence. First, the protein should have reacted with anti-6-kDa-protein serum and/or one of the other antisera (in the case of polyproteins); and second, the immunoreactive proteins should have been detected only with extracts from TEV-His6-infected plants. With anti-6-kDa-protein serum, two polypeptides were detected from extracts of plants infected by TEV-His6 but not wild-type TEV (Fig. 2A). The smaller and more abundant species migrated during electrophoresis to approximately the same position as the synthetic protein used for antiserum production and likely corresponded to the mature, His-tagged 6-kDa protein. The larger species migrated slightly more slowly than purified CI protein. With anti-CI serum also, this polypeptide was detected from TEV-His6 extracts but not extracts from wild-type-TEV-infected plants (Fig. 2B). The larger protein, therefore, was concluded to be the CI/6 polyprotein. The differences in signal intensities of these proteins most likely reflect differences in relative abundance in vivo, although it is possible that accessibility of the His tag to the affinity matrix was limited in the CI/6 polyprotein.

Two proteins were detected specifically from TEV-His6 extracts with anti-NIa serum (Fig. 2C). The larger product migrated during electrophoresis to a position corresponding to that of the 6/NIa polyprotein. The smaller protein, with an apparent molecular mass of 32 kDa, likely corresponded to a polyprotein consisting of the His-tagged 6-kDa protein and the VPg domain of NIa, although the theoretical molecular mass of the 6/VPg polyprotein was 27 kDa. This product would form by proteolytic cleavage at the internal, suboptimal cleavage site in NIa (19). Neither of these putative polyproteins was detected with anti-6-kDa-protein serum (Fig. 2A), perhaps be-

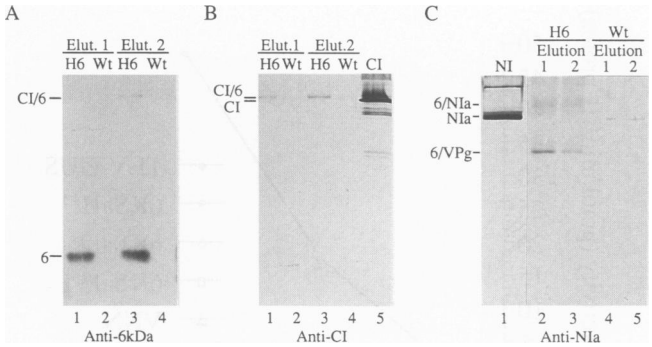

FIG. 2. Analysis of the 6-kDa protein and 6-kDa-protein-containing polyproteins by affinity chromatography. Immunoblots were prepared with aliquots from the first two elution fractions (Elut. 1 and Elut. 2) from Ni^{2+}-NTA columns loaded with extracts from wild-type (Wt) or His-tagged (H6) TEV. The blots were probed with anti-6-kDa-protein serum (A), anti-CI serum (B), or anti-NIa serum (C). Purified CI and NI proteins are shown in panels B and C, respectively. The electrophoretic positions of different polypeptides are indicated to the left of each blot. The immunoblot shown in panel C was prepared with extracts different from those used for panels A and B.

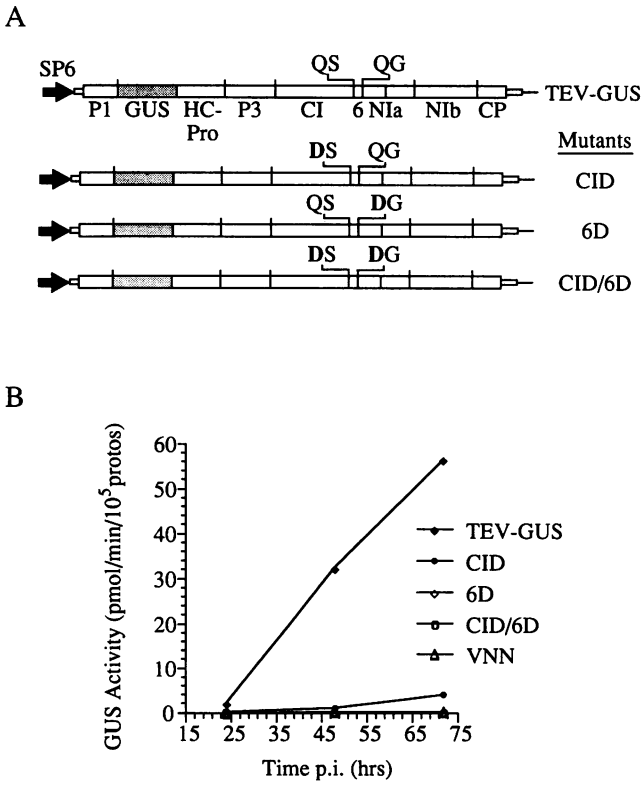

FIG. 3. Diagrammatic representation of 6-kDa protein cleavage site mutants and their amplification in protoplasts. (A) Relevant portions of four plasmids used for the preparation of TEV RNA transcripts. The single-letter codes for the P1 (−1) and P1′ (+1) positions around the cleavage sites between CI and the 6-kDa protein, and between the 6-kDa protein and NIa, are shown above the maps. The mutant Asp (D) residues in the P1 positions are indicated in boldface. (B) Amplification of parental and mutant transcripts in tobacco protoplasts. GUS activity (pmol of substrate cleaved per min per 10^5 protoplasts [protos]) was measured at 24, 48, and 72 h p.i. These data are averages for two independent, contemporaneous transfections from one of three fully replicated experiments.

cause of a relatively low antibody titer. Alternatively, the 6-kDa protein may have lost immunoreactivity as a result of linkage of the NIa sequence to its C terminus. In fact, immunoprecipitation experiments using fusion proteins synthesized in vitro revealed that the 6-kDa protein loses immunoreactivity when viral or nonviral proteins are linked specifically to its C terminus (data not shown).

Involvement of the 6-kDa protein in viral RNA amplification. To address the role of the 6-kDa protein in virus replication, mutations affecting the 6-kDa protein and its N- and C-terminal cleavage sites were generated in the TEV genome and their effects were analyzed in the tobacco protoplast system. The mutations were introduced into a modified variant of TEV derived from transcripts of pTEV7DA-GUS, which specifies a virus encoding GUS as a reporter protein. The GUS sequence was engineered between the P1 proteinase and HC-Pro coding regions such that polyprotein processing would yield a stable GUS–HC-Pro fusion protein in infected cells (15). GUS activity was shown previously to be an effective surrogate marker for viral RNA amplification in TEV-GUS-infected protoplasts (12). As a control to assay for the level of GUS activity stimulated only by the input genomes, a replication-defective mutant (from pTEV7DA-GUS/VNN) containing a change of sequences coding for the highly conserved Gly-Asp-Asp motif to those coding for Val-Asn-Asn in NIb polymerase (12) was also tested in all experiments.

Both the N- and C-terminal cleavage sites flanking the 6-kDa protein were inactivated, either singly or in combination, by mutagenesis of the Gln codon to an Asp codon specifying the P1 position residue (−1 relative to the scissile bond) (Fig. 3A). Substitution of Asp for Gln in the P1 position was shown previously to inactivate NIa-mediated cleavage site function (17). Transcripts were generated from *Bgl*II-linearized parental and mutant plasmids and introduced into protoplasts, and samples were assayed for GUS activity at 24, 48, and 72 h p.i. Parental TEV-GUS stimulated increases of GUS activity at each time point (Fig. 3B). The 6D mutant encoding a defective 6/NIa cleavage site, and the double CID/6D mutant encoding defective sites at the CI/6 and 6/NIa junctions, induced no GUS activity over time and were indistinguishable from the replication-defective, VNN mutant control. The CID mutant, on the other hand, stimulated GUS activity that increased over 72 h, although only to a level approximately 10% as high as that with parental TEV-GUS.

To test the effects of changes within the 6-kDa protein, sequences coding for Ser-Arg-Pro (SRP) tripeptides were inserted at three positions in the 6-kDa protein coding region in pTEV7DA-GUS (Fig. 4A). The 6-kDa protein consists of a highly conserved hydrophilic N-terminal domain, a hydrophobic central region, and a moderately hydrophilic C-terminal domain. The 6-kDa protein encoded by the 6KSal1 mutant contained the SRP insertion after residue 9 in the N-terminal region and possessed a predicted hydropathic character similar to that of the wild-type protein (Fig. 4B). The 6KSal2 mutant encoded a protein with the SRP insertion after position 27, which decreased the predicted local hydrophobic character of the central region. The insertion in the 6KSal3 mutant after residue 37 decreased the predicted hydrophobic property near the end of the central region. Transcripts from each plasmid were introduced into protoplasts, and GUS activity was assayed over 72 h. In contrast to parental TEV-GUS, none of the mutant genomes stimulated GUS activity at any time point above the trace levels induced by the replication-defective

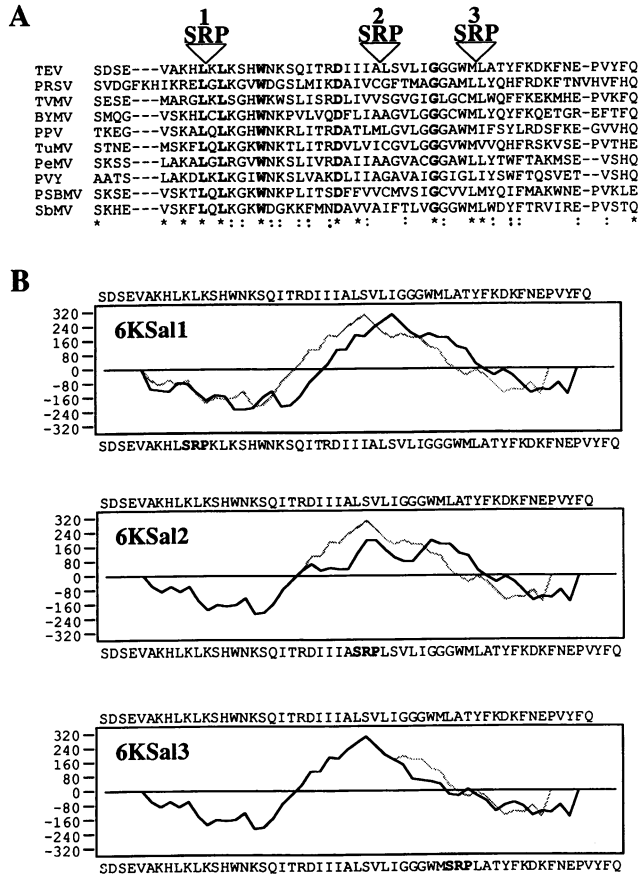

FIG. 4. Alignment of the 6-kDa protein sequences from different potyviruses and hydrophobicity profiles of 6-kDa protein insertion mutants. (A) Alignment of the 6-kDa protein sequences of TEV, papaya ringspot virus (PRSV), tobacco vein mottling virus (TVMV), bean yellow mosaic virus (BYMV), plum pox virus (PPV), turnip mosaic virus (TuMV), pepper mottle virus (PeMV), potato virus Y (PVY), pea seed-borne mosaic virus (PSBMV), and soybean mosaic virus (SbMV). Strictly conserved residues are indicated in boldface with an asterisk below the sequences. Positions in which all sequences contain a structurally conserved residue are indicated by an asterisk. Positions with structurally conserved residues in 7 of 10 sequences are indicated by colons. Dashes represent gaps in the alignment. The positions of the Ser-Arg-Pro (SRP) insertions in the 6KSal1 (1), 6KSal2 (2), and 6KSal3 (3) mutants are indicated above the alignment. (B) Computer-generated hydropathy plots of the wild-type and mutant TEV 6-kDa proteins. The wild-type sequence is indicated above each plot, while the mutant sequence is written underneath, with the insertion in boldface. The wild-type sequence is plotted with a shaded line, while the mutant sequences are plotted with a solid line. The Kyte and Doolittle algorithm (28) was used, with a window of 11 amino acid residues.

VNN mutant (Fig. 5). These results suggested that disruptions within the 6-kDa protein and around the 6-kDa protein cleavage sites were detrimental to TEV-GUS RNA amplification.

Considering the possibility that the amplification-defective phenotypes of the insertion mutants might have been due to restricted accessibility of the 6-kDa protein cleavage sites to proteinase, NIa-mediated proteolysis of modified 6/NIa-containing polyproteins synthesized in a rabbit reticulocyte lysate system was analyzed. The three mutations were introduced

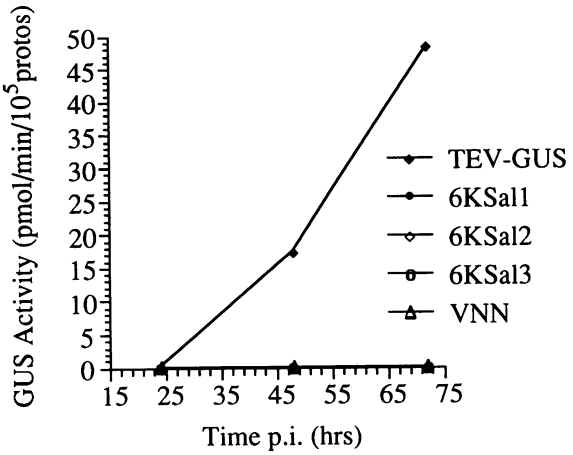

FIG. 5. Amplification of parental and 6-kDa protein insertion mutant transcripts in tobacco protoplasts. GUS activity (pmol of substrate cleaved per min per 10^5 protoplasts [protos]) was measured at 24, 48, and 72 h p.i. These data are averages for two independent, contemporaneous transfections from one of three fully replicated experiments.

into pTL7SN-5471, which encodes a 63-kDa polyprotein consisting of a short segment of CI, the entire 6-kDa protein and NIa sequences, and a small region of NIb (Fig. 6A). The polyprotein encoded by transcripts from nonmutagenized

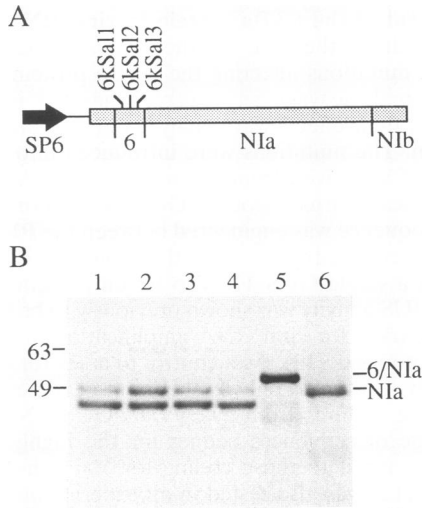

FIG. 6. Synthesis and processing of polyproteins containing mutant 6-kDa protein. (A) Diagrammatic representation of relevant portions of pTL7SN-5471, which was used for insertion of the Ser-Arg-Pro coding sequence. Transcripts from this plasmid encode a 63-kDa polyprotein containing short segments of the CI and NIb proteins, in addition to complete 6-kDa (6) and NIa proteins. The approximate positions of the insertions are indicated above the map. (B) Total translation products from transcripts derived from nonmutagenized pTL7SN-5471 (lane 1), pTL7SN-5471/6KSal1 (lane 2), pTL7SN-5471/6KSal2 (lane 3), pTL7SN-5471/6KSal3 (lane 4), pTL7SN-6/NIaC-A (lane 5), and pTL7SN-49K (lane 6). Transcripts from pTL7SN-6/NIaC-A and pTL7SN-49K encode the 6/NIa polyprotein and the NIa protein, respectively (41, 42). Approximate molecular masses (in kilodaltons) of the polyprotein and processed NIa are shown on the left. Note that NIa undergoes further proteolytic processing to yield a product lacking approximately 2 kDa from its C terminus (39).

pTL7SN-5471 underwent proteolysis to yield NIa (49 kDa) (Fig. 6B, lane 1). A substantial proportion of NIa was also processed further to a 47-kDa form, which may lack approximately 2 kDa from the C terminus (39). Each of the three mutant-derived polyproteins was processed to yield the same 47- and 49-kDa products (Fig. 6B, lanes 2 to 4), indicating that the insertions had little if any effect on cleavage between the 6-kDa protein and NIa. In this in vitro translation and processing assay, however, we were unable to ascertain the effects on proteolysis between the CI and 6-kDa proteins, as the 6-kDa protein was not detected, even after cleavage of the wild-type polyprotein (data not shown).

Subcellular localization properties of the 6-kDa protein. Previous studies indicated that the 6-kDa protein, when linked with NIa in a 6/NIa polyprotein, retarded nuclear translocation of NIa (42). This effect required linkage of the two proteins within a polyprotein, as NIa translocation was activated after autoproteolytic removal of the 6-kDa protein. One hypothesis states that the transport-inhibiting activity of the 6-kDa protein is due to binding to an insoluble cytoplasmic complex or structure. To characterize the subcellular localization properties of the 6-kDa protein, fractionation and immunolocalization analyses with transgenic plants expressing fusion proteins consisting of GUS and the 6-kDa protein were conducted. Analysis of TEV-infected tissue by similar techniques was limited by low levels of immunoreactive 6-kDa protein (see above). The GUS fusion strategy permitted sensitive detection and quantitation of proteins in the fractionation experiments by a fluorometric assay.

Three transgenic plants, expressing nonfused GUS, 6/GUS fusion protein, and GUS/6 fusion protein, were used for the fractionation analysis (Fig. 7A). Cytosolic (S30) and crude membrane (P30) fractions were isolated from leaf tissue. Virtually all of the GUS activity from plants expressing the nonfused reporter protein was associated with the S30 fraction (Fig. 7B). In contrast, at least 90% of the activity from plants expressing either fusion protein was associated with the crude membrane-containing P30 fraction (Fig. 7C and D). Of the 6/GUS and GUS/6 fusion protein associated with the P30 fraction, virtually all was solubilized by treatment with NP-40 (Fig. 7C and D), a nonionic detergent with membrane-solubilizing activity. These data suggest that the 6-kDa protein mediates an association with membranes.

To localize the site of accumulation of nonfused GUS and one of the fusion proteins, GUS/6, at a resolution higher than is permitted by the fractionation analysis, immunogold electron microscopy was conducted. Leaf tissue from young transgenic plants was fixed and embedded in LR White resin, sectioned, and probed with preimmune or anti-GUS serum and a gold particle-linked second antibody. Preimmune serum did not specifically label any particular organelle or structure, although nonspecific reactivity was seen occasionally over nuclei and chloroplasts in many sections tested (Fig. 8A and E). Nonfused GUS induced no unusual cytological abnormalities and was localized primarily to the cytoplasm (Fig. 8B).

Cells from plants expressing GUS/6 fusion protein exhibited three unusual structures not observed in GUS-expressing cells. First, spiral, membrane-like proliferations that often encircled granular material were seen in close proximity to the nucleus (Fig. 8C and D). Second, laminate, membrane-like proliferations at the nuclear envelope were observed consistently in all sections (Fig. 8D through F). In some cases, the spiral structures were clearly contiguous with the apparent membranous proliferations at the nuclear envelope (Fig. 8D). A third structure with the appearance of layers of compacted mitochondria was also seen in several specimens. Each of these

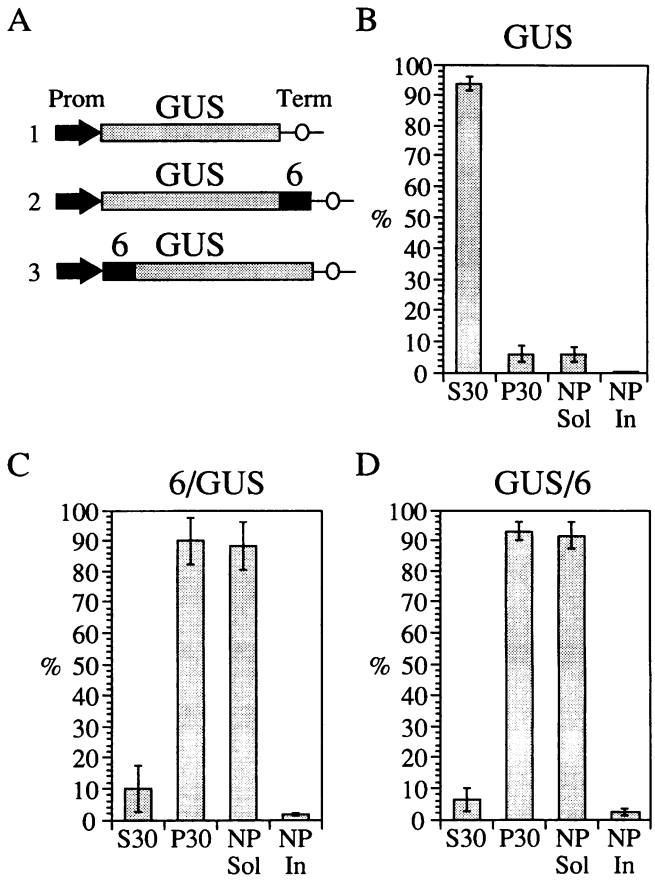

FIG. 7. Subcellular fractionation of GUS and 6/GUS and GUS/6 fusion proteins from transgenic plants. (A) Diagrammatic representation of relevant portions of plasmids expressed in transgenic plants. The cauliflower mosaic virus 35S promoter (Prom) is indicated by an arrow, and the termination and polyadenylation signal (Term) is indicated by an open circle. The GUS coding sequence is indicated by a shaded box, while the 6-kDa protein coding region is indicated by a solid black box. (B, C, and D) Fractionation of GUS and GUS fusion proteins. The percentage of total GUS activity divided between the cytosolic (S30) and the crude membrane (P30) fractions is plotted in the first two columns in each panel. The amounts of NP-40-soluble (NP Sol) and NP-40-insoluble (NP In) activities recovered from the P30 fraction are shown as percentages of total activity in the last two columns in each panel. Standard deviations are indicated by error bars.

novel structures was specifically labeled with anti-GUS serum but not with preimmune serum (Fig. 8C through F). In the case of the apparent mitochondrial aggregates, only the spaces between the compacted mitochondria were labeled (Fig. 8D). These data suggest that cells expressing the 6-kDa protein are induced to form novel membranous structures and that these structures are sites of accumulation of the transgenic protein.

DISCUSSION

The TEV 6-kDa protein and several 6-kDa-protein-containing polyproteins were identified in extracts from infected plants. This was facilitated by use of an engineered variant of TEV encoding a His-tagged 6-kDa protein, enabling concentration of the proteins from relatively large amounts of tissue by Ni^{2+} affinity chromatography. The His tag modification appears to have a neutral effect on the biochemical activities of most proteins (e.g., see reference 24) and thus may be partic-

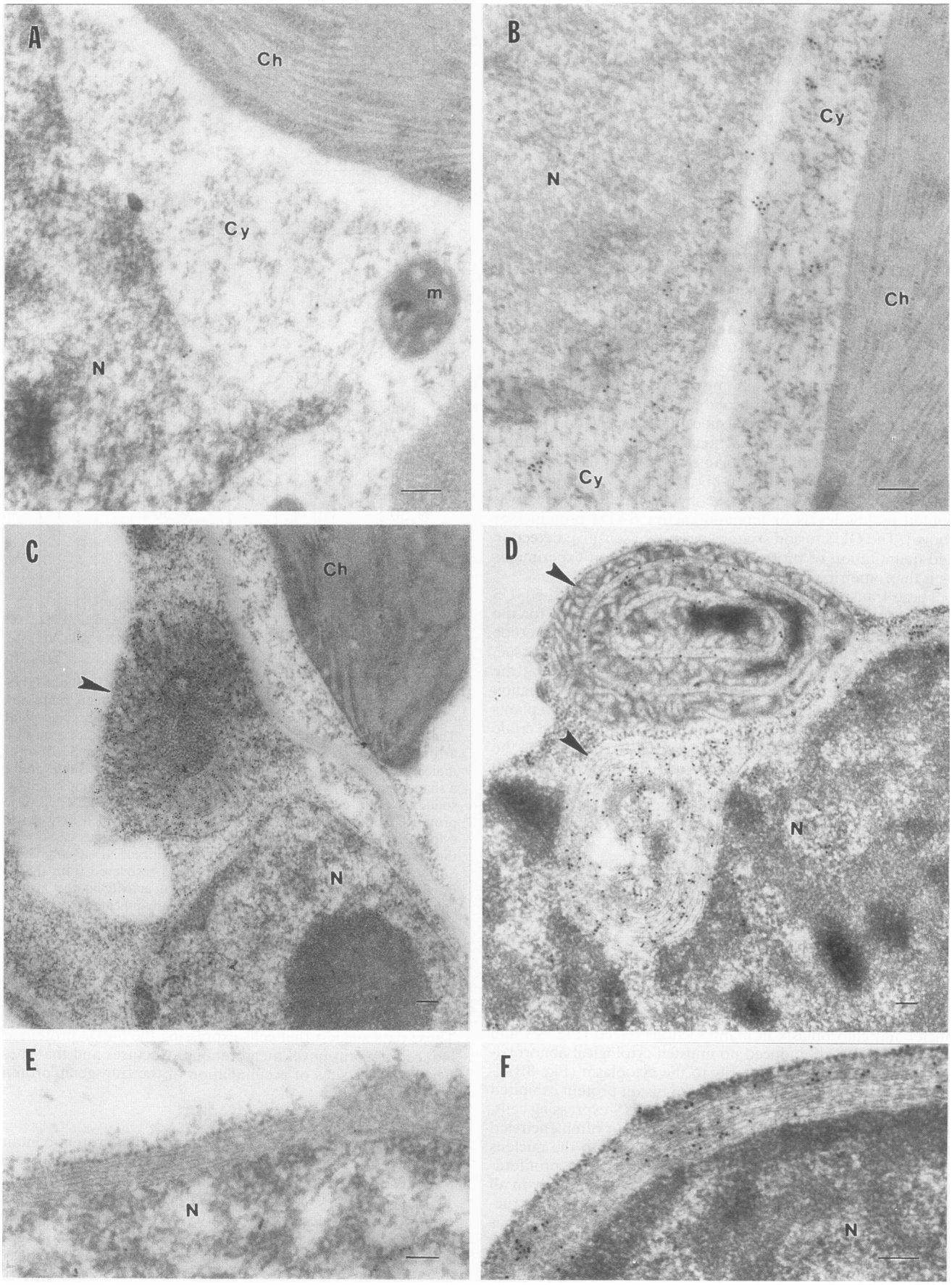
A
Ch
Cy
m
N
B
Cy
N
Ch
Cy
C
Ch
N
D
N
E
N
F
N

ularly useful for analysis of viral proteins present in low concentrations in infected cells. Although denatured proteins were analyzed in this study, Ni^{2+} affinity chromatography works well with native proteins and may be useful for isolation of viral protein complexes formed in vivo.

The detection of free 6-kDa protein indicates that both N- and C-terminal cleavage sites flanking the 6-kDa protein are utilized in vivo. On the basis of the debilitated phenotypes of the 6-kDa protein cleavage site mutants in protoplasts, it is suggested that functional processing sites on both sides of the 6-kDa protein are necessary for efficient virus replication. Interestingly, the CID mutant, containing a defective cleavage site between the CI protein and the 6-kDa protein, induced reporter protein (GUS) activity to 10% of the level induced by the parental virus. Considering that no secondary cell-to-cell spread of virus occurs in the protoplast system, it is highly unlikely that the amplified genomes were revertants, as this would have required the simultaneous independent acquisition of reversion mutations in viral RNAs in at least 10% of transfected cells. This putative mass reversion also would have had to occur soon after transfection, as GUS activity was detected at both 24 and 48 h p.i.

Detection of CI/6 and 6/NIa polyproteins in plants infected by the His-tagged TEV suggests that alternative processing pathways may be used to excise the 6-kDa protein. Due to *cis*-preferential processing of the CI/6 cleavage site in vitro (8), it is proposed that CI/6 polyprotein possesses a relatively long half-life. The function of this polyprotein in the TEV replicative cycle is not clear, although it is predicted to be a membrane-bound RNA helicase on the basis of the activities of the CI (30) and 6-kDa (this study) proteins. The CI protein has been demonstrated to be associated with various membranes, including the plasma membrane in the vicinity of plasmodesmata, during the early stages of infection and prior to formation of cylindrical, cytoplasmic inclusion bodies (3, 31–33). The membrane-binding form of CI might, therefore, be the CI/6 polyprotein. Alternatively, this polyprotein may be a dead-end processing product or a nonfunctional, long-lived intermediate in the proteolytic cascade.

The 6/NIa polyproteins are intriguing in light of the requirement for VPg function in cytoplasmic or membrane-bound replication complexes. Given that full-length NIa and the VPg domain of NIa contain nuclear localization information (11), the presence of the 6-kDa protein sequence within a polyprotein may direct a proportion of NIa to a membrane. In a previous study (42), the 6-kDa protein was shown to override the nuclear transport activity of NIa, presumably by mediating a membrane association as shown here. Comparisons between the 6/NIa polyproteins and the picornavirus 3AB polyprotein may be highly relevant. Both contain a membrane-associated domain (the 6-kDa protein and 3A) and a VPg domain (NIa and 3B). Both can undergo further proteolytic processing to yield VPg free of the membrane-binding protein. In the case of picornaviruses, this processing event was proposed to be concomitant with VPg-primed initiation of RNA synthesis (47). As suggested for 3A protein of picornaviruses (46, 47, 52), the potyviral 6-kDa protein may be one determinant that anchors replication complexes to a membrane. Extensive subcellular fractionation and in situ localization experiments with poliovirus-infected cells (reviewed in reference 47), and limited subcellular fractionation data with plum pox potyvirus-infected leaves (34), have demonstrated that viral RNA replication complexes are membrane associated. If a 6-kDa-protein-containing VPg polyprotein is the active form involved in TEV RNA synthesis, it is possible that both 6/NIa and 6/VPg are functional, as both full-length and internally processed NIa forms have been detected on TEV genomic RNA (12, 36). That 6-kDa-protein-containing polyproteins larger than 6/NIa, such as CI/6/NIa, also function during RNA synthesis cannot be discounted, especially given that the CID mutant containing the cleavage site defect between CI and the 6-kDa protein possessed partial replicative competence.

The absence of GUS activity after transfection of protoplasts with mutant TEV-GUS transcripts encoding 6-kDa proteins with 3-amino-acid insertions strongly suggests that the 6-kDa protein and/or polyprotein is involved in RNA amplification. While a disabling effect on the 6-kDa protein is proposed as the most likely reason for the mutant phenotypes, it is formally possible that the lack of GUS activity reflects a requirement of the 6-kDa protein in TEV RNA translation. This seems unlikely in view of the strong cap-independent, translation-enhancing properties of the TEV 5′ nontranslated sequence in plant cells, an activity that does not require the 6-kDa protein (10). It is also theoretically possible that the lack of activity of the insertion mutants was due to interference with NIa-mediated proteolytic processing of the 6-kDa protein. The in vitro processing activity between the mutant 6-kDa protein and NIa was unaffected in polyproteins containing each insertion. We could not assess the effects on processing at the cleavage site between the CI and 6-kDa proteins. It is doubtful that the inactive phenotypes were due solely to interference at this site, however, as the CID mutant containing a defective CI/6 processing site still expressed reporter protein activity in protoplasts at a level approximately 10% that of parental TEV-GUS. Finally, it is conceivable that the inactive phenotypes were the result of disruption of RNA sequences or structure necessary for RNA replication, although the equally disabling effects of the insertions at three independent positions argues against this possibility.

No biochemical functions other than membrane-binding activity have been ascribed to the 6-kDa protein. The putative RNA amplification defects, therefore, may have been due to debilitation of its membrane-binding function. The insertions may have interfered directly with an interaction between the 6-kDa protein and membrane lipids or proteins, or they may have affected a potential posttranslational modification necessary for the 6-kDa protein-membrane association. The central region of the TEV 6-kDa protein contains a 19-amino-acid hydrophobic domain flanked by hydrophilic Arg-Asp and Lys-Asp dipeptide sequences on either side. This region, which is structurally conserved in all potyvirus 6-kDa proteins, may function as an anchor by insertion directly into the lipid bilayer, although its relatively short length suggests that it does not span the membrane (13). An integral interaction between the 6-kDa protein (or a structure resulting from posttranslational modification) and the lipid bilayer is consistent with the

FIG. 8. Immunogold localization of GUS and GUS/6 in transgenic plant cells. Thin sections were treated first with preimmune or anti-GUS serum and then with a second antibody conjugated to 10-nm gold particles. (A and B) GUS-expressing transgenic plant cells labeled with preimmune (A) or anti-GUS (B) serum. (C through F) GUS/6 fusion protein-expressing transgenic plant cells labeled with preimmune (E) or anti-GUS (C, D, and F) serum. The arrowheads in panels C and D indicate apparent membranous proliferations or mitochondrial aggregates. Bars, 100 nm. Abbreviations: Ch, chloroplasts; N, nucleus; m, mitochondria; Cy, cytoplasm.

solubilization of 6/GUS and GUS/6 fusion proteins by nonionic detergent. However, these experiments do not rule out the possibility that the 6-kDa protein interacts peripherally with the polar exterior of the lipid bilayer or a membrane-associated cellular protein.

Expression of GUS/6 fusion protein in transgenic plants resulted in remarkable membrane-like proliferations with which the fusion protein was associated. Infection of cells by numerous plant and animal viruses results in various types of membrane or vesicular proliferation, and in the case of poliovirus, the induced structures have been shown to be sites of viral RNA synthesis (5). In potyvirus-infected cells, proliferations of endoplasmic reticulum and aggregation of organelles are common (33). In fact, the apparent mitochondrial aggregates observed in this study closely resemble those seen in cells infected by TEV and other potyviruses (23, 26, 33). This suggests that the 6-kDa protein is responsible for induction of at least some of these cytopathic structures.

To our knowledge, the spiral and nuclear envelope-associated membrane-like proliferations have not been reported in TEV-infected cells. These may form as a result of constitutive expression of the membrane-associated fusion protein over long periods and through multiple developmental stages of the transgenic plant. Interestingly, these structures bear a striking resemblance to "karmellae," which are induced in yeast cells that overexpress 3-hydroxy-3-methylglutaryl coenzyme A, an integral membrane protein of the endoplasmic reticulum (54). Karmellae are characterized by up to 10 stacked layers of paired membranes surrounding the nucleus and often extending into the cytoplasm. It was proposed that yeast cells possess a mechanism to sense excess levels of certain membrane proteins and to induce compensatory membrane biogenesis. In the case of viral infection or overproduction of individual viral proteins, proliferation of membranes may be due also to blockage of normal membrane trafficking or recycling. Others have proposed that poliovirus specifically blocks a step in the flow of transport vesicles from the endoplasmic reticulum to the intermediate compartment or the Golgi apparatus and that the vesicles are recruited as the scaffold for RNA replication (35). The proliferation of membrane in response to the 6-kDa protein reported here may reflect a similar diversion of the host endomembrane system during potyvirus infection.

ACKNOWLEDGMENTS

We thank Tom McKnight for supplying the anti-GUS serum, Kate VandenBosch for advice with electron microscopy, and Bill Dougherty for initially bringing to our attention the utility of His tagging.

This research was supported by grants from the National Institutes of Health (AI27832) and the Samuel Roberts Noble Foundation, Inc.

REFERENCES

1. **Allison, R., R. E. Johnston, and W. G. Dougherty.** 1986. The nucleotide sequence of the coding region of tobacco etch virus genomic RNA: evidence for the synthesis of a single polyprotein. Virology **154**:9–20.
2. **An, G.** 1986. Development of plant promoter expression vectors and their use for analysis of differential activity of nopaline synthase promoter in transformed tobacco cells. Plant Physiol. **81**:86–91.
3. **Baunoch, D., P. Das, and V. Hari.** 1988. Intracellular localization of TEV capsid and inclusion proteins by immunogold labeling. J. Ultrastruct. Mol. Struct. Res. **99**:203–212.
4. **Baunoch, D. A., P. Das, M. E. Browning, and V. Hari.** 1991. A temporal study of the expression of the capsid, cytoplasmic inclusion and nuclear inclusion proteins of tobacco etch potyvirus in infected plants. J. Gen. Virol. **72**:487–492.
5. **Bienz, K., D. Egger, and L. Pasamontes.** 1987. Association of polioviral proteins of the P2 genomic region with the viral replication complex and virus-induced membrane synthesis as visualized by electron microscopic immunocytochemistry and autoradiography. Virology **160**:220–226.
6. **Carrington, J. C., S. M. Cary, and W. G. Dougherty.** 1988. Mutational analysis of tobacco etch virus polyprotein processing: *cis* and *trans* proteolytic activities of polyproteins containing the 49-kilodalton proteinase. J. Virol. **62**:2313–2320.
7. **Carrington, J. C., S. M. Cary, T. D. Parks, and W. G. Dougherty.** 1989. A second proteinase encoded by a plant potyvirus genome. EMBO J. **8**:365–370.
8. **Carrington, J. C., and W. G. Dougherty.** 1987. Processing of the tobacco etch virus 49K protease requires autoproteolysis. Virology **160**:355–362.
9. **Carrington, J. C., and W. G. Dougherty.** 1987. Small nuclear inclusion protein encoded by a plant potyvirus genome is a protease. J. Virol. **61**:2540–2548.
10. **Carrington, J. C., and D. D. Freed.** 1990. Cap-independent enhancement of translation by a plant potyvirus 5′ nontranslated region. J. Virol. **64**:1590–1597.
11. **Carrington, J. C., D. D. Freed, and A. J. Leinicke.** 1991. Bipartite signal sequence mediates nuclear translocation of the plant potyviral NIa protein. Plant Cell **3**:953–962.
12. **Carrington, J. C., R. Haldeman, V. V. Dolja, and M. A. Restrepo-Hartwig.** 1993. Internal cleavage and *trans*-proteolytic activities of the VPg-proteinase (NIa) of tobacco etch potyvirus in vivo. J. Virol. **67**:6995–7000.
13. **Darnell, J. E., H. F. Lodish, and D. Baltimore.** 1986. Molecular cell biology. Scientific American Books, New York.
14. **Dolja, V. V., and J. C. Carrington.** 1992. Evolution of positive-strand RNA viruses. Semin. Virol. **3**:315–326.
15. **Dolja, V. V., H. J. McBride, and J. C. Carrington.** 1992. Tagging of plant potyvirus replication and movement by insertion of β-glucuronidase into the viral polyprotein. Proc. Natl. Acad. Sci. USA **89**:10208–10212.
16. **Domier, L. L., J. G. Shaw, and R. E. Rhoads.** 1987. Potyviral proteins share amino acid sequence homology with picorna-, como-, and caulimoviral proteins. Virology **158**:20–27.
17. **Dougherty, W. G., J. C. Carrington, S. M. Cary, and T. D. Parks.** 1988. Biochemical and mutational analysis of a plant virus polyprotein cleavage site. EMBO J. **7**:1281–1287.
18. **Dougherty, W. G., and E. Hiebert.** 1980. Translation of potyvirus RNA in a rabbit reticulocyte lysate: identification of nuclear inclusion proteins as products of tobacco etch virus RNA translation and cylindrical inclusion protein as a product of the potyvirus genome. Virology **104**:174–182.
19. **Dougherty, W. G., and T. D. Parks.** 1991. Post-translational processing of the tobacco etch virus 49-kDa small nuclear inclusion polyprotein: identification of an internal cleavage site and delimitation of VPg and proteinase domains. Virology **183**:449–456.
20. **Giachetti, C., S. S. Hwang, and B. L. Semler.** 1992. *cis*-Acting lesions targeted to the hydrophobic domain of a poliovirus membrane protein involved in RNA replication. J. Virol. **66**:6045–6057.
21. **Giachetti, C., and B. L. Semler.** 1991. Role of a viral membrane polypeptide in strand-specific initiation of poliovirus RNA synthesis. J. Virol. **65**:2647–2654.
22. **Harlow, E., and D. Lane (ed.).** 1988. Antibodies, laboratory manual, p. 53–138. Cold Spring Harbor Laboratories, Cold Spring Harbor, N.Y.
23. **Harrison, B. D., and I. M. Roberts.** 1971. Pinwheels and crystalline structures induced by atopa mild mosaic virus, a plant virus with particles 925 nm long. J. Gen. Virol. **10**:71–78.
24. **Janknecht, R., G. D. Martynoff, J. Lou, R. A. Hipskind, A. Nordheim, and H. G. Stunnenberg.** 1991. Rapid and efficient purification of native histidine-tagged protein expressed by a recombinant vaccinia virus. Proc. Natl. Acad. Sci. USA **88**:8972–8976.
25. **Jefferson, R. A.** 1987. Assaying chimeric genes in plants: the GUS gene fusion system. Plant Mol. Biol. Rep. **5**:387–405.
26. **Kitajima, E. W., and O. Lovisolo.** 1972. Mitochondrial aggregates in datura leaf cells infected with henbane mosaic virus. J. Gen. Virol. **16**:265–271.

27. **Kunkel, T. A., J. D. Roberts, and R. Zakour.** 1987. Rapid and efficient site-specific mutagenesis without phenotypic selection. Methods Enzymol. **154**:367–382.
28. **Kyte, J., and R. F. Doolittle.** 1982. A simple method for displaying the hydropathic character of a protein. J. Mol. Biol. **157**:105–132.
29. **Laín, S., M. T. Martín, J. L. Riechmann, and J. A. García.** 1991. Novel catalytic activity associated with positive-strand RNA virus infection: nucleic acid-stimulated ATPase activity of the plum pox potyvirus helicase protein. J. Virol. **65**:1–6.
30. **Laín, S., J. L. Riechmann, and J. A. García.** 1990. RNA helicase: a novel activity associated with a protein encoded by a positive-strand RNA virus. Nucleic Acids Res. **18**:7003–7006.
31. **Langenberg, W. G.** 1986. Virus protein association with cylindrical inclusions of two viruses that infect wheat. J. Gen. Virol. **67**:1161–1168.
32. **Lawson, R. H., and S. S. Hearon.** 1971. The association of pinwheel inclusions with plasmodesmata. Virology **44**:454–456.
33. **Lesemann, D.-E.** 1988. Cytopathology, p. 179–235. *In* R. G. Milne (ed.), The plant viruses. IV. The filamentous plant viruses. Plenum Publishing Corporation, New York.
34. **Martín, M. T., and J. A. García.** 1991. Plum pox potyvirus RNA replication in a crude membrane fraction from infected *Nicotiana clevelandii* leaves. J. Gen. Virol. **72**:785–790.
35. **Maynell, L. A., K. Kirkegaard, and M. W. Klymkowsky.** 1992. Inhibition of poliovirus RNA synthesis by brefeldin A. J. Virol. **66**:1985–1994.
36. **Murphy, J. F., R. E. Rhoads, A. G. Hunt, and J. G. Shaw.** 1990. The VPg of tobacco etch virus RNA is the 49 kDa proteinase or the N-terminal 24 kDa part of the proteinase. Virology **178**:285–288.
37. **Murphy, J. F., W. Rychlik, R. E. Rhoads, A. G. Hunt, and J. G. Shaw.** 1990. A tyrosine residue in the small nuclear inclusion protein of tobacco vein mottling virus links the VPg to the viral RNA. J. Virol. **65**:511–513.
38. **Negrutiu, I., R. Shillito, I. Potrykus, G. Biasini, and F. Sala.** 1987. Hybrid genes in the analysis of transformation conditions. I. Setting up a simple method for direct gene transfer in plant protoplasts. Plant Mol. Biol. **8**:363–373.
39. **Parks, T. D., and W. G. Dougherty.** 1993. Personal communication.
40. **Quadt, R., and E. M. J. Jaspars.** 1990. Purification and characterization of brome mosaic virus RNA-dependent RNA polymerase. Virology **178**:189–194.
41. **Restrepo, M. A., D. D. Freed, and J. C. Carrington.** 1990. Nuclear transport of plant potyviral proteins. Plant Cell **2**:987–998.
42. **Restrepo-Hartwig, M. A., and J. C. Carrington.** 1992. Regulation of nuclear transport of a plant potyvirus protein by autoproteolysis. J. Virol. **66**:5662–5666.
43. **Reynolds, E. S.** 1963. The use of lead citrate at high pH as an electron opaque stain in electron microscopy. J. Cell Biol. **17**:208–213.
44. **Riechmann, J. L., S. Laín, and J. A. García.** 1989. The genome-linked protein and 5′ end RNA sequence of plum pox potyvirus. J. Gen. Virol. **70**:2785–2789.
45. **Riechmann, J. L., S. Laín, and J. A. García.** 1992. Highlights and prospects of potyvirus molecular biology. J. Gen. Virol. **73**:1–16.
46. **Semler, B. L., C. W. Anderson, R. Hanecak, L. F. Dorner, and E. Wimmer.** 1982. A membrane-associated precursor to poliovirus VPg identified by immunoprecipitation with antibodies directed against a synthetic heptapeptide. Cell **28**:405–412.
47. **Semler, B. L., R. J. Kuhn, and E. Wimmer.** 1987. Replication of the poliovirus genome, p. 23–48. *In* J. Holland, E. Domingo, and P. Ahlquist (ed.), RNA genetics. CRC Press, Inc., Boca Raton, Fla.
48. **Shahabuddin, M., J. G. Shaw, and R. E. Rhoads.** 1988. Mapping of the tobacco vein mottling virus VPg cistron. Virology **163**:635–637.
49. **Strauss, E. G., J. H. Strauss, and A. J. Levine.** 1990. Virus evolution, p. 167–190. *In* B. N. Fields, D. M. Knipe, R. M. Chanock, M. S. Hirsch, J. L. Melnick, T. P. Monath, and B. Roizman (ed.), Virology. Raven Press, New York.
50. **Suzuki, N., T. Kudo, Y. Shirako, Y. Ehara, and T. Tachibana.** 1989. Distribution of cylindrical inclusion, amorphous inclusion and capsid proteins of watermelon mosaic virus 2 in systemically infected pumpkin leaves. J. Gen. Virol. **70**:1085–1091.
51. **Takegami, T., R. J. Kuhn, C. W. Anderson, and E. Wimmer.** 1983. Membrane-dependent uridylation of the genome-linked protein VPg of poliovirus. Proc. Natl. Acad. Sci. USA **80**:7447–7451.
52. **Takegami, T., B. L. Semler, C. W. Anderson, and E. Wimmer.** 1983. Membrane fractions active in poliovirus RNA replication contain VPg precursor polypeptides. Virology **128**:33–47.
53. **Verchot, J., E. V. Koonin, and J. C. Carrington.** 1991. The 35-kDa protein from the N-terminus of a potyviral polyprotein functions as a third virus-encoded proteinase. Virology **185**:527–535.
54. **Wright, R., M. Basson, L. D'Ari, and J. Rine.** 1988. Increased amounts of HMG CoA-reductase induce "karmellae": a proliferation of stacked membrane pairs surrounding the yeast nucleus. J. Cell Biol. **107**:101–114.